

Filaments of Crime: Informing Policing via Thresholded Ridge Estimation

Ben Moews · Jaime R. Argueta, Jr. · Antonia Gieschen

Abstract

Objectives We introduce a new method for reducing crime in hot spots and across cities through ridge estimation. In doing so, our goal is to explore the application of density ridges to hot spots and patrol optimization, and to contribute to the policing literature in police patrolling and crime reduction strategies.

Methods We make use of the subspace-constrained mean shift algorithm, a recently introduced approach for ridge estimation further developed in cosmology, which we modify and extend for geospatial datasets and hot spot analysis. Our experiments extract density ridges of Part I crime incidents from the City of Chicago during the year 2018 and early 2019 to demonstrate the application to current data.

Results Our results demonstrate nonlinear mode-following ridges in agreement with broader kernel density estimates. Using early 2019 incidents with predictive ridges extracted from 2018 data, we create multi-run confidence intervals and show that our patrol templates cover around 94% of incidents for 0.1-mile envelopes around ridges, quickly rising to near-complete coverage. We also develop and provide researchers, as well as practitioners, with a user-friendly and open-source software for fast geospatial density ridge estimation.

Conclusions We show that ridges following crime report densities can be used to enhance patrolling capabilities. Our empirical tests show the stability of ridges based on past data, offering an accessible way of identifying routes within hot spots instead of patrolling epicenters. We suggest further research into the application and efficacy of density ridges for patrolling.

Keywords Hot Spots, Density Ridge Estimation, Patrol Routes, Policing

Mathematics Subject Classification (2010) 62G07 · 62H11 · 62P25

1 Introduction

Previous research on spatial crime patterns acknowledges the general stability of crimes within a concentrated geographic area (Weisburd et al, 2004; Groff et al, 2010). Within these concentrated areas, or hot spots, most investigations of policing tactics find that concentrated efforts on problem areas are an effective means of reducing crime (Sherman and Weisburd, 1995; Braga and Weisburd, 2010; Braga et al, 2014). Other approaches to investigating crime reduction strategies study the efficacy of patrolling strategies. Koper (1995) and Telep et al (2014)

Ben Moews
Institute for Astronomy, University of Edinburgh
Royal Observatory, Edinburgh, EH9 3HJ, UK
E-mail: b.moews@ed.ac.uk

Jaime R. Argueta, Jr.
School of Criminal Justice, University of Cincinnati
2600 Clifton Ave, Cincinnati, OH 45221, USA
E-mail: arguetjr@mail.uc.edu

Antonia Gieschen
Business School, University of Edinburgh
29 Buccleuch Place, Edinburgh, EH8 9JS, UK
E-mail: antonia.gieschen@ed.ac.uk

contribute to the patrol literature through a time-based investigation, finding that 15 minutes of police presence in a given hot spot significantly decrease both calls for service and Part I crime incidents. These recent practices suggest that the stability of places and efficiency of patrols allow for an optimization of tactics. Specifically, one way to optimize patrol routes is through a focus on temporal and spatial aspects of hot spots, decreasing the latter while still providing a presence to the community (Camacho-Collados and Liberatore, 2015).

Practitioners and police officers rely on spatial analytics to identify hot spots to dictate their patrols. Common practices of identifying hot spots involve kernel density estimation (KDE), spatial ellipses, grid-thematic mapping, or the Getis-Ord G_i^* statistic (Chainey et al, 2008a; Ratcliffe, 2010). These techniques share the commonality of identifying a wide problem area with little regard to specific problem places, and an over-reliance on the applied bandwidth to identify the epicenter of a given hot spot (Eck et al, 2005). In doing so, the planning of specific patrol routes is left to the discretion of the police department. Recently, density ridge estimation has become a focal topic in statistics and a variety of application areas. The mathematics behind density ridge estimation aims to construct ridges that follow high-density areas, or modes, of a distribution, allowing for higher-dimensional extensions (Ozertem and Erdogmus, 2011; Chen et al, 2015a).

Previous scholars have explored patrol route optimization through a variety of techniques such as multi-agent-based simulations, for example Fukunaga and Hostetler (1975), machine learning as in Li et al (2011) and Marchant et al (2018), and graph theory and evolutionary computing (Chawathe, 2007; Al Boni and Gerber, 2016). These studies consistently illustrate that route optimization is a feasible task, and agencies can apply advanced methods that account for resources and time. The primary issues among these methods are their complexity and limited application. In addition, the use of complex analytics to optimize route efficiency ignores the basic patrol services to the greater community.

For this reason, the present study seeks to address the previous shortcomings of patrol optimization by applying methods from neighboring disciplines. We focus on and extend the subspace-constrained mean shift algorithm presented by Ozertem and Erdogmus (2011) in order to introduce the concept of density ridges to the field of criminology. The identification of ridges will allow law enforcement to methodologically patrol hot spots, address surrounding areas, and reduce calls for service. With this method, the application of ridge identification is available for public use by agencies and researchers alike. This study uses Chicago Part I crime incident data from 2018 to develop and illustrate the application of ridge estimation, and data from early 2019 to test for predictive accuracy in coverage, as well as for convergence consistency, with multi-run confidence intervals to account for subsampling.

The remainder of this paper is structured as follows. Section 2 provides an overview of the current literature that revolves around modeling patrol strategies, as well as applications of density ridge estimation in other fields and motivations arising from the latter. Section 3 details data sources, methodology, software implementation, and analytic recommendations that are required to conduct the proper analyses and estimate optimal ridges, while Section 4 documents the results and provides illustrations to understand the advantages and disadvantages of optimizing patrol routes. Finally, Section 5 discusses limitations and implications, provides an overview of the optimization for patrolling ridges as opposed to other patrol strategies, and compares our approach to related research, followed by Section 6 concluding our work.

2 Literature Review

This section reviews previous scholarly findings on hot spots, patrol optimization, and applications of ridge estimation in other fields. Several methodological approaches and applications on how to best estimate the kernel density of high-crime areas have been suggested for agency use. This section covers the pertinent literature on hot spots in Sec. 2.1, followed by relevant background on patrol optimization in Sec. 2.2. Lastly, Sec. 2.3 describes previous related research on applications of the core algorithm used in this paper in other fields.

2.1 Hot Spots

Sherman et al (1989) report that about 3.3% of street addresses produce over half of the calls for service in Minneapolis. Since then, numerous other scholars found large numbers of calls for service concentrating in small areas in a given city, generally reaching up to 5% (Sherman and Weisburd, 1995; Braga et al, 2014). In related research, Weisburd et al (2004) find that hot spots chronically persist for longer than a decade in 5% of block-long

street segments. Based on this, Wilcox and Eck (2011) coined the phenomenon of a concentration of the hottest segments as ‘The Iron Law of Troublesome Places’, while Weisburd (2015) refers to the same concept as the ‘Law of Crime Concentration’. Subsequent work also finds that hot spots vary in size for different types of crimes and are generally stable in their locations, for example gun crimes as reported by Braga et al (2010), robberies as in Braga et al (2012), and all other major crimes (Telep et al, 2014; Haberman, 2017).

Empirical evidence from these studies enables researchers and applications in two major ways. The first is testing techniques on stable hot spots and investigating which policing strategies can be most effective for problem places. Secondly, this research sparked varying measures and techniques to identify the concentration of crime at places from a macro or micro perspective. A variety of hot spot policing tactics has been used and evaluated since the recognition of the success in hot spots policing. Importantly, Braga (2007) finds that patrolling hot spots does not disperse crime to neighboring geographic locations. Instead, deterrent effects are diffused to nearby streets, making the concentration of efforts in patrolling hot spots a successful endeavor (Braga, 2005; Braga et al, 2014). Ratcliffe et al (2011) report, for a randomized trial, that focused police intervention in the form of foot patrols reduces violent crime by 23% in target hot spots. The remaining tactics find significant reductions in crime when focusing on specific places. In summary, hot spot policing provides a notable strategy for police departments to effectively reduce crimes by patrolling micro-places (Sherman et al, 1989; Weisburd et al, 2004; Weisburd and Telep, 2011).

In this context, Haberman (2017) presents research on overlapping hot spots. Importantly, the findings suggest that if police were to try to focus on specific crimes such as robberies or assaults, different hot spots would need to be evaluated to combat such problems. This implies the need for police agencies to identify and commit greater resources if they seek to reduce specific crime types. Additionally, a focus on problem places introduces concerns regarding the dosage of patrols and provided attention. Related studies find that patrolling concentrated areas within 15 minutes significantly reduces calls for service within the area (Koper, 1995; Telep et al, 2014). After this time frame, however, the presence of police officers yields diminishing returns in terms of crime reduction, thus wasting police resources. Recently, Linning and Eck (2017) find that weak interventions at problem places, as well as too strong of a focus, can backfire. In other words, if the patrol dosage administered at hot spots is insufficient, offenders may retaliate, adapt, or find new criminal opportunities. Therefore, prior research on hot spots suggests the need for efficient and effective patrol optimization strategies.

2.2 Patrol Optimization

For strategic planning, law enforcement makes use of hot spots to identify problem areas and patrol routes for police. For this reason, the identification of routes in and between hot spots is most relevant due to motor patrols being constrained by street networks (Menton, 2008). Police agencies approach the identification of hot spots through basic statistical methods and tools, as most crime analysts do not have access to advanced statistical knowledge or techniques (Mamalian et al, 1999; Ratcliffe, 2004). Other methods such as the Getis-Ord G_i^* statistic have also been used to detect crime clustering. Within police departments, however, advanced route planning based on proper hot spot estimations still lags behind most current research.

Patrol optimization deals with the identification of optimal routes in such a way that officers target problem places efficiently. In previous research, models address this challenge through, for example, the traveling salesman problem and other approaches (Chevaleyre et al, 2004; Chawathe, 2007; Li et al, 2011). While these methods are complex, they offer the potential to observe how criminals react to patrol routes, or their effects on crime rates. Paruchuri et al (2008) showcase the applicability of dynamic modeling by assuming that offenders will predict patrol routes, demonstrating the ability to determine optimal paths that strike a balance between predictable and unpredictable paths in a street network. Related research suggests a potential to decrease criminal activity and the public’s fear of crime, for example by modeling patrol routes illustrating the shortest Hamiltonian cycle for visiting each location in a city (Chevaleyre, 2004).

Additional facets of patrol optimization take limited patrol resources into consideration. Chawathe (2007) applies patrol optimization that uses a cost-benefit analysis, maximizing the coverage of hot spots and accounting for the paths between streets and places. Similarly, Reis et al (2006) produce a multi-agent-based algorithm to design efficient patrol strategies. Their simulation models a city’s road network to find optimal routes to minimize crime in the city. Further works study changing offender preferences for where to commit criminal activity, and simulate changing problem places that adapt to patrol routes (Melo et al, 2005; Furtado et al, 2006).

Even with progress underway, there are still several limitations that patrol optimization studies fail to consider in their analyses. Previous patrol studies do not account for the community’s desires or the multitude of police activities that pull officers away from predetermined routes. Ignoring temporal, spatial, and other constraints of police duties also deprives researchers of the ability to apply their research in realistic scenarios. Put simply, the deterministic fashion of covering entire patrol areas or deploying algorithms that have the capability of adapting to criminal behavior cannot account the spuriousness of real-time events and patrols. Overall, the modeling of optimal patrol routes and simulated agents to combat problem places and limited resources is still in the early stages. In addition, while valuable for researching the impacts of policing strategies, real-world applications of optimal patrol routes are severely limited.

2.3 Applications of Ridge Estimation

Our approach is an extension of the subspace-constrained mean shift algorithm (SCMS), a density ridge estimation method described in detail in Section 3.2. Since its inception by Ozertem and Erdogmus (2011), the algorithm sparked the interest of various fields to apply ridge estimation to an array of problems, providing insights into its broad applicability. Notably, an extensive adoption of this method to investigate a number of phenomena can be found in cosmology, where it is used to approximate the cosmic web, the organization of the large-scale structure of galaxies in the universe divided by immense voids (Carroll and Ostlie, 2013). Research endeavors dealing with the latter application, especially with regard to extensions like thresholding, also have a significant influence on the work presented in this paper.

Chen et al (2015b) propose the use of the SCMS algorithm to detect filamentary structures in the cosmic web, pointing out its suitability to constrain the distribution of matter at different redshifts to explore the evolution of the Universe. Redshift, in this context, refers to different distances corresponding to different times due to the distance light has to travel (Hubble, 1929). They also show how the algorithm can be used to investigate how baryonic matter, meaning what is normally perceived as matter, traces the distribution of dark matter, a hypothetical form of matter that interacts only gravitationally and is thought to account for most of the matter present in our Universe (Chen et al, 2015c).

This methodological investigation is followed-up in Chen et al (2016) with an application of their approach to construct a catalog of filaments using Sloan Digital Sky Survey data (York et al, 2000). In addition, the algorithm is used to explore the effect of the distance to the nearest filament on galaxy properties such as a galaxy’s age, size, stellar mass, and color (Chen et al, 2017). In yet another take on utilizing ridge estimation for cosmology, He et al (2017) apply the SCMS algorithm to study the non-Gaussianity of the Universe’s matter density field, providing the first detection of filament-based gravitational lensing effects, meaning the bending of light via gravitation exerted by matter, in the cosmic microwave background.

While the difference between the fields of cosmology and criminology may seem insurmountable at first, abstracted problems and the applicability of mathematical techniques often span areas of research, allowing for the common exchange of methodology between them. Following this tradition of cross-field pollination, these applications to the structure of the cosmic web provide a motivation for the SCMS algorithm’s application to crime patterns. Much like the interest in cosmology to identify and constrain filaments in order to gain insights into large-scale structures, the identification of such high-density filaments offers a way to extract route templates useful for police patrol optimization. In astrophysics, the SCMS algorithm is also used to identify morphological substructures for the classification of stellar debris, aiding in the investigation of galactic mergers through the disruptions left behind by the collision of galaxies (Hendel et al, 2018).

Apart from research in cosmology and astrophysics, the SCMS algorithm has found various other areas of application such as neuroimaging (Bas and Erdogmus, 2011). Bas and Erdogmus (2011) introduce a method to analyze images of neuron structures by using KDE for density estimation and tracing ridges of these estimates via the SCMS algorithm. The objective of their study is the extraction of curvilinear structures from three-dimensional neuronal tissue images. A key aspect for this application is the connectivity between structures that is present in their data. Their method is able to trace these tree-like structures in neuronal image data by providing the algorithm with an initial seed and direction for tracing the principal curves.

This flexibility of the algorithm to trace tree-like structures as well as curvilinear lines is further exploited by Miao et al (2014) to identify road networks from images, with their objective being the extraction of smooth road centerlines. For this, they use an approach based around SCMS, in combination with tensor voting and the

geodesic method to improve the computational efficiency of the algorithm, as is required by their application scenario, showing that even complex roadmaps can be extracted using this approach. The applicability to patrol routes is, in this case, easy to see, as density ridges can provide templates to which road networks can subsequently be mapped.

A closely related approach to the SCMS algorithm has also been developed in the context of facial image recognition. It is used for marking and tracking so-called landmarks in images of faces, a technique introduced by Saragih et al (2009). Based on this, Kaashki and Safabakhsh (2018) use the algorithm for fitting their model to recognize and identify three-dimensional pictures of faces. Shreve et al (2014) also use this technique for spotting micro and macro facial expressions in videos. The tracking of facial landmarks in pictures or videos can, however, not only be used for the identification of persons or expressions, as Zamzmi et al (2018) show by introducing a way of suppressing facial expressions to improve information retrieval, for example for face recognition algorithms. By using the algorithm to automatically detect and track 66 facial landmarks, they are able to show especially good suppression results for strong expressions such as happiness.

3 Data and Methods

This section covers the data used in this work, as well as the mathematical background, extensions and modifications, and software implementation of our approach in preparation for our experiments. Sec. 3.1 describes our data and the corresponding preprocessing, as well as our choice and use of the data. Following this, Sec. 3.2 provides a theoretical overview of the subspace-constrained mean shift algorithm as a core foundation of this paper, whereas Sec. 3.3 covers appropriate distance measures. In Sec. 3.4, we describe our modifications and extensions of the core algorithm to make it a suitable tool for our work, and end with introducing an open-source tool for practitioners in Sec. 3.5.

3.1 Crime Incident Data

Datasets suitable for our work need to fulfill certain criteria to be of interest to both researcher and practitioner communities: In order to facilitate the reproducibility of our results, the dataset has to be easily accessible, without restrictions, as open-source data that can be used by interested readers to confirm and build on our work. The data also have to be very recent for the results to be of interest to practitioners. With these constraints in mind, we make use of the Chicago Data Portal^a, an open-access data service of the City of Chicago. The portal features a complete dataset of reported crime incidents from 2001 to the present day, covering over 17 years, with the exception of murders where data exist for each victim. The crime incident data are provided by the Citizen Law Enforcement Analysis and Reporting (CLEAR) system of the Chicago Police Department and, which is important for our choice of this source, is updated in fast-enough intervals to contain a complete subset for the year 2018.

After obtaining the dataset, we extract all entries pertaining to that most recent full year, and retain only three variables of interest; the primary crime type as well as the latitude and longitude values of the reported crime's location. After this step, which ensures that the subsequent deletions only affect entries that feature missing data in relevant variables, we omit all entries for which one of the three retained variables is not present. This omission for missing data leads to the data for 2018 being reduced from 178,659 to 177,669 entries, resulting in a negligible loss of around 0.5% of data points.

In this work, we focus on Part I offenses as defined by the Uniform Crime Reports^b (UCR), a national official crime data compilation of the Federal Bureau of Investigation (Reid, 1979). Our choice of Part I crimes reflects both the high priority placed on this type of crime and the reliability of this type of information to illustrate the crime rates within a given city (Barnett-Ryan et al, 2014). In this context, aggravated assault, forcible rape, criminal homicide, and robbery are Part I violent crimes, whereas arson, burglary, larceny-theft and motor vehicle theft are Part I property crimes. We extract these eight primary types from the preprocessed dataset, which leaves us with 78,894 incidents of Part I crimes in Chicago during the year 2018, an overview of which is provided in Tab. I. In order to keep our algorithm's runtime low, and given that we are interested in keeping the overall density

^a <https://data.cityofchicago.org/>

^b <https://www.ucrdatatool.gov/>

Table I. Part I crime incident numbers for Chicago during the year 2018.

Primary crime type	Number of data points
Larceny-theft	42,423
Aggravated assault	13,843
Burglary	7,821
Motor vehicle theft	6,641
Robbery	6,525
Forcible rape	1,013
Criminal homicide	386
Arson	242

As present in data from the Chicago Data Portal. Different primary crime types are listed separately, with entries sorted by the number of reported incidents in descending order.

profile of crime incidents, we use uniformly-random sampling to further reduce the dataset to 5,000 data points to provide a use case relatable to many application cases.

3.2 Subspace-Constrained Mean Shift

In order to provide readers with the background of the employed method, a short overview of the mathematical foundations is required. Given a probability density function $p : \mathbb{R}^d \rightarrow \mathbb{R}$ of dimensionality d , as well as a corresponding gradient $\nabla p(x)$ and a Hessian $H(x)$, let $v = \{v_1, v_2, \dots, v_d\}$ be the eigenvectors of $H(x)$ corresponding to eigenvalues $\lambda = \{\lambda_1, \lambda_2, \dots, \lambda_d\}$ sorted in descending order. Defining $\Delta(x)$ as the diagonal matrix with λ along the diagonal, and with the eigendecomposition $H(x) = U(x)\Delta(x)U(x)^\top$, we let v' be the columns of $U(x)$ associated with the $d - 1$ smallest entries in λ . In addition, let $L(x) \propto L(H(x)) = v'v'^\top$ be a projection on the linear space of the columns in v' , then the projected gradient is defined as $\nabla p(x) = L(x)g(x)$. For a map $\xi : \mathbb{R} \rightarrow \mathbb{R}^d$, the ridge R can be expressed as $R = \{x : \|G(x)\| = 0, \lambda_{d+1}(x) < 0\}$. In other words, a density ridge is a local density maximization in the normal direction given by the Hessian. While the above provides a bare-bones definition, we refer the interested reader to Genovese et al (2014) for a more detailed introduction to non-parametric ridge estimation.

Kernel density estimation, which is also known as the Parzen-Rosenblatt window, is a non-parametric statistical method to estimate probability density functions (Rosenblatt, 1956; Parzen, 1962). For a given smoothing kernel \mathcal{K} , a multidimensional KDE for a point x , the number of dimensions d , and a dataset θ can be computed as:

$$\text{KDE}(x, \beta) = \frac{1}{|\theta|\beta^d} \sum_{i=1}^{|\theta|} \mathcal{K}\left(\frac{\|x - \theta_i\|}{\beta}\right) \quad (1)$$

The most common choice is the radial basis function (RBF) kernel, also known as the Gaussian kernel, with $\mathcal{K}(x) = (1/\sqrt{2\pi}) \exp(-0.5x^2)$. Using the latter, Eq. 1 can be rewritten as follows:

$$\text{KDE}_{\text{RBF}}(x, \beta) = \frac{1}{|\theta|(2\pi\beta^2)^{\frac{d}{2}}} \sum_{i=1}^{|\theta|} e\left(\frac{\|x - \theta_i\|^2}{2\beta^2}\right) \quad (2)$$

Ozertem and Erdogmus (2011) first introduce the subspace-constrained mean shift algorithm, a KDE-based non-parametric iterative approach to estimate the ridges of a probability density function in the context of self-consistent smooth curves using $\nabla p(x)$ and $H(x)$. This method is extended with thresholding by Chen et al (2015b) for the application to cosmic web reconstruction, using a KDE over the dataset to counteract the effect of areas with low probability densities. Previous research on facial image recognition by Saragih et al (2009) introduces a closely related approach that, while mathematically different and used for facial landmark identification, includes multiple features of the SCMS algorithm as well as the same descriptor, although written slightly differently as ‘subspace constrained mean-shifts’. The SCMS algorithm, including the latter extension and with a Gaussian smoothing kernel, is described in a formalized version in Alg. 1.

Algorithm 1 SCMS with thresholding

```

1: Input: Coordinates  $\theta$ , bandwidth  $\beta$ , threshold  $\tau$ , iterations  $N$ 
2: Output: Density ridge point coordinates  $\psi$ 
3: procedure SCMS( $\theta, \beta, \tau, N$ )
4:    $\kappa(x) \leftarrow \text{KDE}_{\text{RBF}}(\theta, \beta)$ , using Eq. 2
5:    $\psi \leftarrow \psi \sim U((\min(\theta_{*,1}), \max(\theta_{*,1})), (\min(\theta_{*,2}), \max(\theta_{*,2})))_{|\theta|}$ 
6:    $\psi \leftarrow \forall y \in \psi : \kappa(y) < \tau$ 
7:   for  $n \leftarrow 1, 2, \dots, N$  do
8:     for  $i \leftarrow 1, 2, \dots, |\psi|$  do
9:       for  $j \leftarrow 1, 2, \dots, |\theta|$  do
10:         $\mu_j = \frac{\psi_i - \theta_j}{\beta^2}$ 
11:         $\sigma_j = \mathcal{K}_{\text{RBF}}\left(\frac{\psi_i - \theta_j}{\beta}\right)$ 
12:      end for
13:       $H(x) = \frac{1}{|\theta|} \sum_{j=1}^{|\theta|} \sigma_j \left(\mu_j \mu_j^\top - \frac{1}{\beta^2} \mathbb{I}\right)$ 
14:       $v, \lambda \leftarrow v, \lambda$  from eigendecomposition  $\text{eig}(H(x))$ 
15:       $v' \leftarrow$  entries in  $v$  corresponding to  $\text{sort}_{\text{asc}}(\lambda)_{1,2,\dots,d-1}$ 
16:       $\psi_i \leftarrow v' v'^\top \frac{\sum_{j=1}^{|\psi|} \sigma_j \theta_j}{\sum_{j=1}^{|\psi|} \sigma_j}$ 
17:    end for
18:  end for
19:  return  $\psi$ 
20: end procedure

```

Ghassabeh et al (2013) analyze the convergence properties of the SCMS algorithm and show that the method inherits some properties of the previous mean shift algorithm by Fukunaga and Hostetler (1975), most importantly its monotonicity and the convergence of density estimates along the output sequence, together with other properties that offer theoretical guarantees for stopping criteria. For an up-to-date contextualization of the approach in the broader field of topological data analysis, we refer the reader to Wasserman (2018), as well as to Qiao and Polonik (2016) for a more general analysis of non-parametric density ridge estimation. In addition, an investigation of the uncertainty of estimated density ridges through bootstrapping-based confidence sets can be found in Chen et al (2013), and Genovese et al (2012) provide a study of, as well as extensive proofs for, ridge estimation from a geometrical perspective. The SCMS approach of Ozertem and Erdogmus (2011) also finds applications in dimensionality reduction via manifold learning, a type of nonlinear dimensionality reduction, as described in Li and Kwong (2014).

3.3 Geospatial Distance Measures

While the Euclidean distance is a staple in geometric calculations, its use can lead to distorted measures when applied to geospatial coordinates. The reason behind this caveat is that distances in practical use cases involving latitude-longitude coordinates are traversed along the spheroidal body of our planet (Chrisman, 2017). In this context, the orthodromic distance is the shortest path between two coordinates on a sphere, measured along the sphere's surface. As such, it provides a sufficiently realistic way to calculate distances as geodesics on an approximated shape of the Earth. For an array θ of two coordinates with latitudes $\theta_{*,1}$ and longitudes $\theta_{*,2}$ in the first and second column, respectively, let $\Delta\theta_1$ and $\Delta\theta_2$ be the absolute differences of latitudes and longitudes. In this case, the central angle $\Delta\sigma$ can be calculated as:

$$\Delta\sigma = \cos^{-1}(\sin \theta_{1,1} \sin \theta_{2,1} + \cos \theta_{1,1} \cos \theta_{2,1} \cos \Delta\theta_2) \quad (3)$$

The haversine function of an angle α , which is better-conditioned for small geodesic distances, is defined as:

$$\text{hav}(\alpha) = \frac{1 - \cos(\alpha)}{2} = \sin^2\left(\frac{\alpha}{2}\right) \quad (4)$$

The haversine formula, a term coined by Inman (1835), makes use of Eq. 4 and provides a way to calculate the orthodromic distance suitable for our purposes. Using the above, we can calculate the central angle as follows:

$$\Delta\sigma = \text{hav}^{-1}(\text{hav}(\Delta\theta_1) + \cos \theta_{1,1} \cos \theta_{2,1} \text{hav}(\Delta\theta_2)) \quad (5)$$

With R as the radius of the Earth, and denoting the latitudes and longitudes separately everywhere, the haversine distance between points θ_1 and θ_2 is then:

$$\mathbb{M}_{\text{hav}}(\theta_1, \theta_2) = \text{hav}(\theta_{2,1} - \theta_{1,1} + \cos \theta_{1,1} \cos \theta_{2,1} \text{hav}(\theta_{2,2} - \theta_{1,2})) \quad (6)$$

Given the city-level nature of our work, this distance function offers a suitable approach to measurements. At the same time, it admits the use of our methodology and the software tool introduced in this paper across larger areas without suffering from a loss in accuracy scaling with the area size.

3.4 Modifications and Extensions

In addition to providing a fast pure-Python implementation of the SCMS algorithm by Ozertem and Erdogmus (2011), with thresholding as described by Chen et al (2015b), we introduce multiple modifications of the methodology tailored to geospatial data and applications in criminology.

Williamson et al (1999) introduce an optimal bandwidth calculation for crime incident data, based on the average distance of each coordinate to its nearest k neighbors, averaged over all coordinates in the dataset (Eck et al, 2005). For the distance $\mathbb{M}(\theta_i, \theta_j)$ between two coordinates of a dataset θ , and with the number of nearest neighbors k , the calculation of the optimal bandwidth $\hat{\beta}$ takes the form of the following equation:

$$\frac{1}{k|\theta|} \sum_{i=1}^{|\theta|} \sum_{j=1}^k \mathbb{M}(\theta_i, \theta_j) \quad (7)$$

This approach is related to the k -nearest neighbors (k -NN) algorithm, a non-parametric statistical method commonly applied to regression and classification problems (Cover and Hart, 1967). We make use of this calculation to provide a default bandwidth for our method.

As described in Section 3.3, the haversine formula provides a way to compute the orthodromic distance that is suitable for small distances in relation to the respective sphere's radius. While this is a technically more correct approach to calculate distances on the Earth's surface, this approach also makes our methodology applicable to datasets spanning both city-level regions and larger areas, for example on a national level or across multiple countries. For this reason, we use Eq. 6 and, by extension, the orthodromic distance instead of the Euclidean distance for the KDE that the SCMS algorithm makes use of, allowing us to take the Earth's curvature into account. In addition, we also use this distance for the k -NN approach of calculating an optimal bandwidth, replacing $\mathbb{M}(\theta_i, \theta_j)$ in Eq. 7 with $\mathbb{M}_{\text{hav}}(\theta_i, \theta_j)$ from Eq. 6.

Well-approximated density ridges require the SCMS algorithm to run over a sufficient number of iterations. Since a trial-and-error approach is not the most time-efficient way of using the algorithm, we implement a convergence check that uses the mean shift update in Alg. 1. Let the update be denoted as $\phi_{n,i}$, for iteration n and $j \in \{1, 2, \dots, |\psi|\}$ for ridge candidate points ψ , then the calculation takes the following form:

$$\phi_{n,i} = v' v'^{\top} \frac{\sum_{j=1}^{|\psi|} \sigma_j \theta_j}{\sum_{j=1}^{|\psi|} \sigma_j} - \psi_i \quad (8)$$

We then introduce the convergence criterion, for a convergence threshold c , as the absolute difference between an iteration's current update and the last iteration's update not exceeding the convergence threshold, meaning that $\|\phi_{n-1,i} - \phi_{n,i}\| \leq c$.

Lastly, practitioners in criminology are often primarily interested in hot spots, focusing their efforts on regions with high probability densities. In order to enable this use of our method, we propose a cut-off functionality to return only ridge estimates in regions with a high number of data points in comparison to the dataset. For a given percentage value p , the KDE in the SCMS algorithm is used to only retain ridge estimate points above the $(100 - p)^{\text{th}}$ percentile of the dataset's estimated probability density function. This means that the ridge estimate points ψ are, with the same bandwidth β as before and the Gaussian-kernel KDE described in Eq. 2, reduced to a subset ψ' :

$$\begin{aligned} \psi' &= \hat{\psi} \in \psi : \text{KDE}_{\text{RBF}}(\hat{\psi}, \beta) \geq \gamma, \\ \text{with } \gamma &= \min \left(\text{sort}_{\text{desc}} (\text{KDE}_{\text{RBF}}(\psi, \beta))_{1,2,\dots, \lfloor \frac{p}{100} |\psi| \rfloor} \right) \end{aligned} \quad (9)$$

Table II. Input parameters for DREDGE.

Parameter	Function	Default
coordinates	Spatial data as latitude-longitude coordinates	
*neighbors	Number of nearest neighbors to get a bandwidth	10
*bandwidth	Bandwidth used for kernel density estimates	None
*convergence	Threshold used for inter-iteration convergence	0.01
*percentage	Aimed-for percentage of highest-density ridges	None

Only the first parameter specifying geospatial latitude-longitude coordinates is required as an input. Optional parameters that, if not provided by the user, refer to default values and adaptive behavior of the code, are marked with an asterisk.

This approach allows for the exclusive retention of ridge estimates that fall within regions of high probability densities, effectively slicing the density landscape horizontally at the required percentage level and extracting the ridge estimate points that can be found on the remaining landscape.

3.5 Open-Source Tool for Practitioners

Since we want to provide the research community and practitioners with an easy-to-handle implementation that includes all modifications and extensions described in Section 3.4, as well as to enable the reproduction of our work, we introduce a pure-Python software tool for *density ridge estimation describing geospatial evidence* (DREDGE), written for Python 3. The tool itself is available on, and can be installed via, the Python Package Index (PyPI).^c

One of the primary aims in developing a user-friendly tool is to combine customizability with minimal requirements, allowing for the automated use of default parameters and adaptive code behavior while enabling users to fine-tune in accordance with their needs. For this reason, the only mandatory input of DREDGE is an array of coordinates, with one row per data point and latitudes and longitudes in the first and second column, respectively. Since larger datasets lead to smaller bandwidths via the automatic bandwidth calculation described in Section 3.4, we recommend a set of coordinates numbering between 1,000 and 10,000 samples. In case of larger sample sizes, we advise users to manually set a bandwidth, as explained below. In addition to the input of coordinates, four further parameters can be manually set by the user.

The first optional parameter concerns the number of neighbors used to calculate an optimal bandwidth as described in Eq. 7, which has to be an integer value larger than zero. Smaller values for this parameters result in smaller bandwidths, leading to a more fine-grained map of ridge estimates. The second optional parameter enables users to set the bandwidth directly, with the requirement that the value is a positive real number. Providing this parameter disables the automatic calculation of an optimal bandwidth, forcing the code to use the given value. The third optional parameter is the convergence threshold that controls the termination behavior of the algorithm, with the same requirement of a positive real number. The lower this parameter is set, the stricter the assessment of convergence to smooth filaments becomes, at the cost of an increased runtime.

Lastly, the fourth optional parameter is disabled by default and can be set to any real number from the interval $[0, 100]$, indicating the desired percentage to cut the outputted density ridge estimate points to a subset as described in Eq. 9. If, for example, a value of 10.0 is provided, only ridge estimates above the 90th percentile of the dataset’s approximated probability density function are returned. For a better overview, required and optional input parameters for DREDGE are listed in Tab. II, with optional parameters indicated by an asterisk. All user-provided inputs are checked for compliance with format and data type requirements when calling the tool’s primary function, offering custom error messages in case of an incompatibility for one or more input parameters.

Software tools geared toward both research and their use by practitioners benefit from being well-documented and freely available, allowing users to easily understand and, if necessary, adapt the source code to their needs. Therefore, the complete code for DREDGE is available as open-source software in a public repository^d, accompanied by a quickstart tutorial and a use case featuring example code in the form of a downloadable notebook.

^c <https://pypi.org/>

^d <https://github.com/moews/dredge>

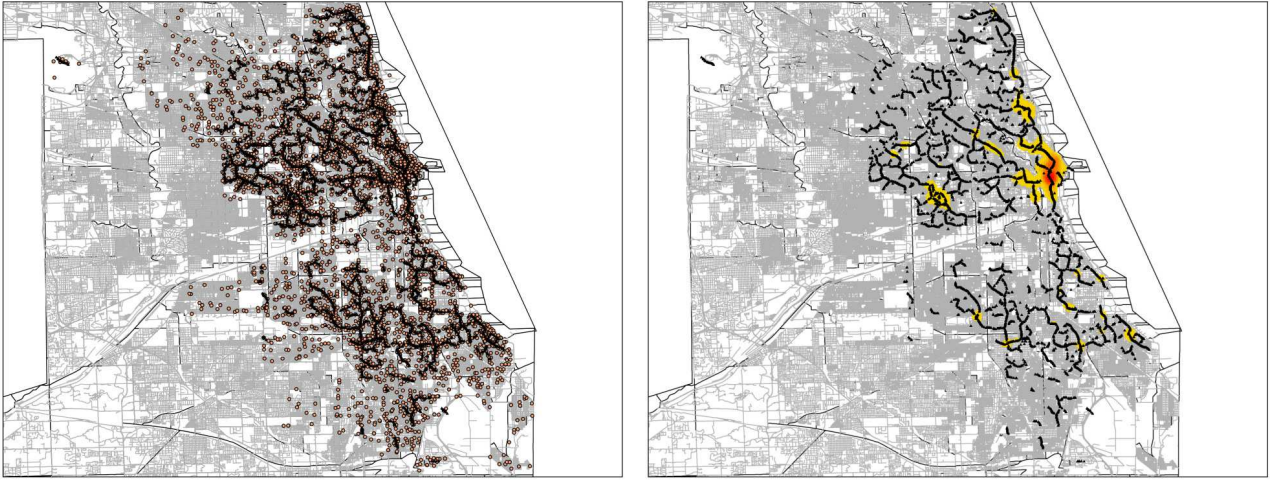


Figure 1. Full density ridges extracted from reported Part I crime incidents for the City of Chicago during 2018. The left panel adds a sample of underlying coordinates, whereas the right panel adds a kernel density estimate (KDE) for the samples in the left panel.

4 Results

In order to make a convincing case for the applicability of our approach, experimental evidence for such a viability is required. While simulated toy examples can be used for such endeavors, stronger evidence is delivered through the application to relevant real-world data. For this purpose, we apply our method to the dataset described in Section 3.1, retrieving density ridges for Part I crimes reported in the City of Chicago in 2018. In doing so, we apply DREDGE to a recent dataset of current interest, providing compelling evidence for our approach. In addition, as outlined in Section 3.1, the dataset is available through the open-access data service of the City of Chicago, the Chicago Data Portal. This, together with the open-source code we provide, facilitates an easy implementation of our results in the spirit of replicability and open science.

The theoretical work on hot spots and direct patrols has been widely applied and studied within the field of criminology (Braga et al, 2014). Current real-world applications of patrol routes include foot and motor patrols that are mainly planned using street network models and KDE (Mamalian et al, 1999; Ratcliffe, 2004). Our work seeks to capitalize on that aspect through density ridge estimation. The density ridges obtained through this experiment with Part I crime incidents for the City of Chicago during 2018 are shown in both panels of Fig. 1. In the left panel, we additionally show a sample of 5,000 coordinates of reported crime incidents, the same size as used by the DREDGE run. In the right panel, we overlay the density ridges with a KDE based on the same optimal bandwidth used by our method, demonstrating the center-line compliance of ridges with hot spots identified by traditional approaches. The implementation of our method described in this paper is run with default values, allowing the software to make use of its adaptive behavior.

The practical application and ease of policing hot spots has allowed police departments to police specific areas more readily (Weisburd and Lum, 2005). Capitalizing on the concentration of problem places, we make use of DREDGE's ability to retrieve density ridges from a specified level of high-density areas, as discussed in Sec. 3.5. Fig. 2 shows the respective top-percentage ridges retrieved through this experiment. Both panels show partial density ridges, making use of the built-in threshold functionality set to 5% for density ridges covering the region above the 95th percentile of the incident density distribution. As in Fig. 1, the left panel additionally shows a sample of 5,000 coordinates of reported crime incidents, the same size as used by the DREDGE run, to show the relation of ridges to the underlying dataset, whereas the right panel overlays the density ridges with a KDE estimate for the data points relevant to the top 5% ridges.

Due to the same underlying analysis, the high-density area highlighted through the KDE visualization in Fig. 1 corresponds to the hot spot singled out in Fig. 2. This location falls within the Near North Side and Loop areas of downtown Chicago, known as being frequented by tourists and large crowds due to shopping districts such as

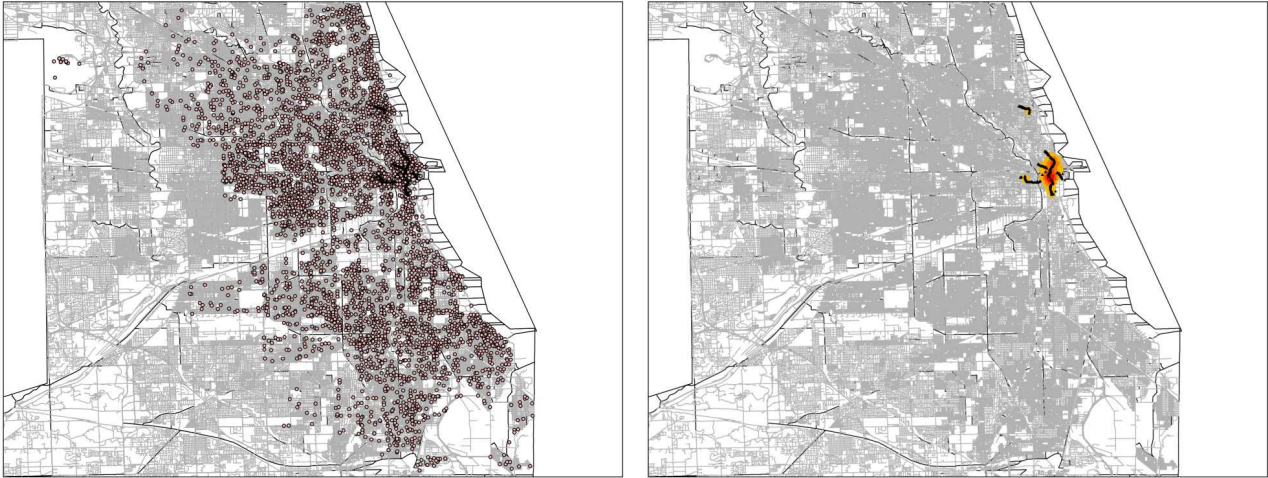


Figure 2. Partial density ridges extracted from reported Part I crime incidents for the City of Chicago during 2018. The left panel adds a sample of underlying coordinates, whereas the right panel adds a kernel density estimate (KDE) for the ridge-related hot spots.

the Magnificent Mile, as well as their nightlife and various landmarks. An obvious interpretation of this high-density accumulation of data points relies on the considerable overrepresentation of larceny-theft in our dataset, as these areas provide ample opportunity for such crimes, combined with scaling effects due to the number of people frequenting them.

In order to empirically test the predictive accuracy and stability of density ridges over time, as well as to verify the subsampling of crime report coordinates, we extract another dataset from the Chicago Data Portal. The procedure remains the same as in Sec. 3.1, but with data for the year 2019 until the end of May 2019, amounting to 38,205 preprocessed Part I crimes. We then treat this new dataset as reported crime incidents, but employ the ridges extracted from the previous 2018 data to simulate route optimization for future policing. For a subsample of crime reports of the same size as before, we measure the distance to the nearest density ridge and calculate the percentage of incidents falling into this envelope around ridges, quantifying the amount of incidents in 2019 that happen near a route template based on 2018 data.

This approach to measuring the effectiveness of our approach is related to a hit rate, meaning the percentage of crime incidents occurring within an area of a certain size (Chainey et al, 2008b). In related work, Bowers et al (2004) propose a search efficiency rate that counts the number of events per square kilometres, although this approach lacks comparability between different study areas. Our choice to measure the percentage of overall crime incidents within envelopes around ridges bears the closest resemblance to the prediction accuracy index (PAI) by Bowers et al (2004). The PAI computes the percentage of crime incidents within a predicted area, divided by the percentual size of the predicted areas in relation to the respective study area. Notably, accounting for the predicted area size is not a concern in our ridge-specific approach, which predicts curvilinear filaments instead of areas. Instead, our measurement's equivalent is the envelope width around ridges, which requires the calculation of the crime incident coverage for varying widths in order to accurately represent the ridges' success.

We compute this experiment for distances in the interval $[0.1, 1]$ in miles, in steps of 0.01 miles, and repeat each experiment for each distance for a total of 10 times, to recover confidence intervals. Each of these 10 runs per distance step is based on a random subsample of reports from the year 2018, with a different random seed each time, to validate the efficacy of a comparatively small subsample of 5,000 data points. In addition, we measure the number of iterations required each time to test the suitability of the convergence criterion introduced in Sec. 3.4.

Fig. 3 shows the results of this experiment. The black line in the primary plot depicts the share of Part I crime reports in the City of Chicago from 2019 data on the vertical axis, depending on the size of the distance envelope around ridges on the horizontal axis. The shaded area around the curve indicates 95% confidence intervals for 10 runs per distance, demonstrating the low variation in coverages for comparatively small subsamples that enable fast runtimes. We expect a concave curve path to reflect a diminished increase in coverage with higher distances,

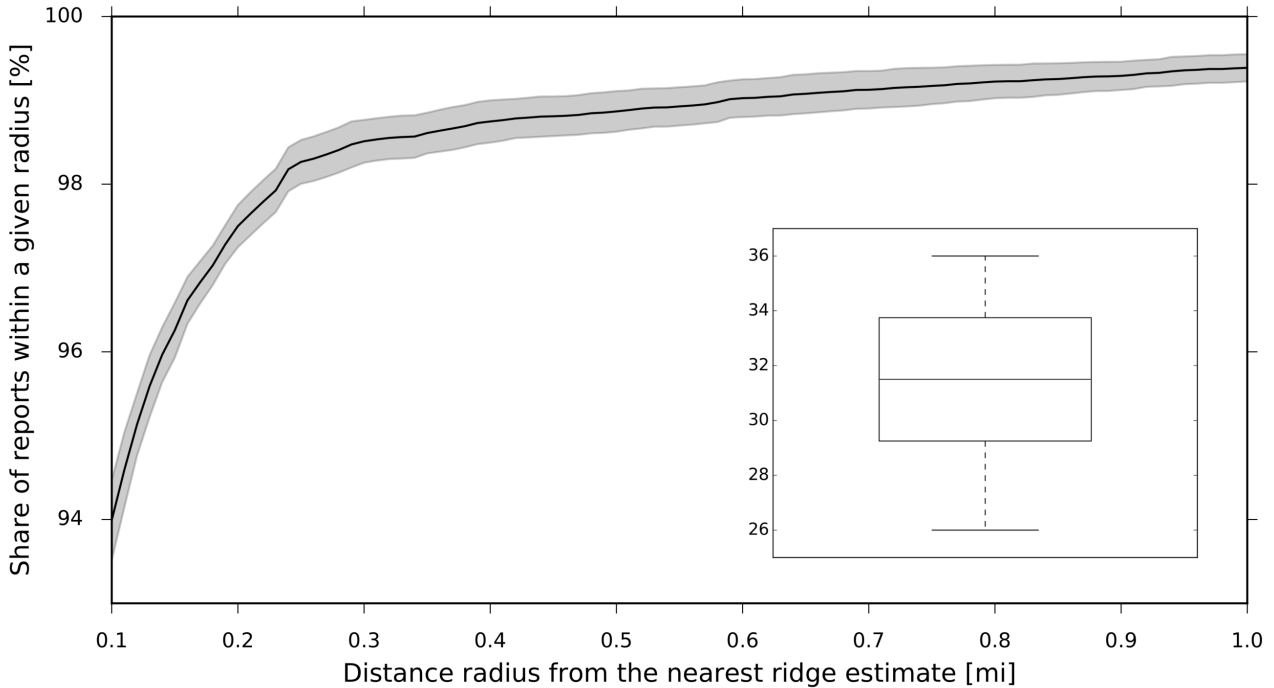


Figure 3. Distance-based coverage for Part I crimes in early 2019 in the City of Chicago, for ridges calculated with data from 2018. The subplot in the lower right corner shows a box-and-whiskers plot for the number of iterations to convergence.

as ridges should closely follow higher-density areas. The curve path in the figure clearly shows this behavior, with ridge envelopes covering 94% of incidents at 0.1 miles, quickly rising to 97.5% and 98.5% at 0.2 and 0.3 miles, respectively, and reaching 99% coverage at about 0.6 miles. In the subplot in the lower right corner of Fig. 3, we show a box-and-whiskers plot, with the upper and lower boundaries of the boxing indicating values within 1.5 times the interquartile range, the horizontal line intersecting the box denoting the median, and the off-standing ‘whiskers’ indicating the minimum and maximum values (McGill et al, 1978). The number of iterations remains stable for different subsamples, demonstrating consistent convergence for subsampled sets in line with the narrow confidence shown in the primary plot.

5 Discussion and Limitations

In this exploratory study, we illustrate a policing method that maximizes patrol efficiency and crime coverage. Based on extensions from the field of cosmology, we make use of the SCMS algorithm for patrol routes within and between hot spots. Our experiments demonstrate the potential impact on patrol route planning, and allow for future research on crime reduction benefits over different populations, periods, and hot spots. Using UCR Part I crimes from the Chicago Data Portal for 2018 and early 2019, our results show the applicability of the presented methods to real-world datasets in contemporary scenarios. These experiments reveal that optimized patrol templates cover about 94% of incidents within 0.1 miles of ridges, reaching to about 99% coverage at 0.6 miles. We implement multiple realizations of our experiments to investigate the stability of crime coverage with predictive ridges based on past data. The corresponding results demonstrate relative stability within narrow confidence intervals across differing subsamples, validating the applicability of our approach for large-scale data.

Research on hot spots maintains that crime concentrates within a small geographic area (Weisburd et al, 2004). The widespread assumption when modeling hot spots is that the epicenter of the hot spots is where police attention should be focused. While the center of a given hot spot may be telling of the most salient problem places, commonly

employed density estimation methods can obscure underlying features (Eck et al, 2005). The epicenter may, for example, be interpreted as a place to heavily patrol in lieu of surrounding areas that may deserve equal or more attention. Thus, this study implies a refutation of previous assumptions about optimal patrol routes within hot spots to reduce crime through deterrent effects. Previous literature observes that police presence provides deterrent effects with regard to offenders who operate on limited information about police deployment patterns or target intervention (Weisburd and Braga, 2019). For this reason, we argue that the use of such a ridge-based optimization strategy can greatly reduce crime within hot spots.

Empirical analyses that use KDE techniques or similar statistical modeling approaches often serve one function, namely guiding patrol routes. While this is critical for analyses of crime reduction strategies, an officer’s duty to serve the community is neglected in the process. Scholars thus should consider accounting for the flexibility and spuriousness of police work. For this reason, our work simplifies patrol routes into segments and priority areas in hot spots. In addition, the benefit of ridges over previous work on patrol routes is the flexibility of the route. In-between duties, this application is not meant to be the primary focus of patrols but rather an addition. Finally, with the open-source availability of our implementation, the application of this program by both researchers and practitioners is feasible.

The identification of crime concentration through spatial analysis allows police officers and agencies to tackle problem places. The issue of the epicenter misleading officers to focus patrols on the central area of a mode is a matter of identifying which places and routes will efficiently deliver deterrence effects. Most crime concentrates within a small area because criminals are most familiar with the routes and buildings surrounding their routine activities (Cohen and Felson, 1979). The place where crime concentrates is thus a stopping point along with their daily lives. Therefore, in lieu of patrolling one stopping point that is criminogenic and identifiable, these ridges utilize the space around the problem places that lead to the epicenter, serving a dual function of patrolling the criminogenic locations and targeting surrounding routes that may encompass their daily activities.

Our study is not without limitations. The methodology applied in this paper does not account for the geometry of street networks, or takes problem places into consideration. In other words, our approach does not apply weights to problem places or the certainty level with which routes may be constrained by the topology or street network of the city. Therefore, future work could focus on the application of spatial weights to problem areas, and on accounting for the topology of the environment. In addition, this work assumes that the organization of patrol routes is implementable solely based on filament optimization, not considering community residents who may want to stop officers or demand more presence (Leigh et al, 2017). Given the fixed location of hot spots, the desires of residents, and the possible need to redraw routes due disruptive calls and city-specific street layout considerations, such alterations should follow an as-close-as-possible alignment with ridges.

While our implementation performs successful density ridge estimation in a matter of minutes, this requires subsampling from larger datasets of coordinates. As a rule of thumb, we recommend to use a minimum of 1,000 and a maximum of 10,000 data points to ensure representativeness and sufficiently fast runtimes. This is due to the algorithm’s complexity being $\mathcal{O}(d \cdot |\theta|^2)$, meaning that it scales linearly with the number of dimensions, which is fixed to $|\theta| = 2$ in our case of latitude-longitude coordinates, but exponentially with the number of data points fed into the algorithm (Ozertem and Erdogmus, 2011). While sample sizes are, in practice, influenced by both time constraints and the size of available datasets, details on effective sample sizes in geospatial dataset resampling can be found in Griffith (2005) and Li et al (2016).

Bias in data is a general problem spanning many fields, which extends to geospatial coordinates. One prominent example is the phenomenon of over- and underpolicing based on previous records, different socioeconomic status, and additional factors such as personal characteristics (Black, 1980). Since our analysis is based on reported crime incidents, one important limitation of our work relates to previous research on disparities in crime reporting. This multi-faceted issue spans both contextual factors in victim and offender characteristics influencing reporting, as demonstrated by Xie and Lauritsen (2012), and localized reluctance of reporting crime incidents (Slocum et al, 2010). For this reason, practical implementations based on such data should always strive to take the risk of biases present in these datasets into account.

6 Conclusion

Optimizing police patrols, both city-wide and with regard to hot spots, remains a topic of interest for researchers and practitioners alike. For this purpose, we show how recent advances in statistics, which are further informed by

applications in cosmology, can be used to detect principal curves, or density ridges, in geospatial crime incident distributions in order to extract high-density paths. With this work, we hope to extend the nature of addressing problem places while tackling the larger hot spot that encompasses it. Problem places can, for example, be addressed before or after route completion such that the overall hot spot is addressed through a deterrence framework. Overall, the impact of this method can potentially provide fruitful gains for future patrol methodologies and applications.

In modifying the subspace-constrained mean shift algorithm in terms of distance measures and the ability to threshold density ridges, we make our methodology suitable for coordinates across arbitrary spatial scales and with hot spots in mind. Our results demonstrate the viability of this approach through locations of reported Part I crime data from the City of Chicago during the year 2018, exemplifying the applicability to patrol route planning and optimization. In using early 2019 reports to test the coverage of these predictive ridges, we observe that the vast majority of crime reports fall into narrow envelopes around them. These experiments also show the viability of our approach for intuitive visualizations, allowing for their combination with knowledge about city-specific traffic routes to plan effective routes. An important feature of our method is the wide applicability to a variety of problems across arbitrary area sizes. In addition, we provide the research community, as well as practitioners, with a user-friendly and customizable open-source software tool to easily access and apply our research.

Acknowledgments

We thank the City of Chicago and the Chicago Police Department for making the data used in this work freely accessible in a well-documented and frequently updated format. We also wish to express our thanks to Nicholas Corsaro, Cory Haberman, and Monsuru Adepeju for helpful suggestions and comments.

References

- Al Boni M, Gerber MS (2016) Automatic optimization of localized kernel density estimation for hotspot policing. In: 15th IEEE International Conference on Machine Learning and Applications, pp 32–38, DOI 10.1109/ICMLA.2016.0015
- Barnett-Ryan C, Langton L, Planty M (2014) The nation’s two crime measures. Tech. rep., Bureau of Justice Statistics & Federal Bureau of Investigation, program report, U.S. Department of Justice, NCJ 246832
- Bas E, Erdogmus D (2011) Principal curves as skeletons of tubular objects. *Neuroinformatics* 9(2):181–191, DOI 10.1007/s12021-011-9105-2
- Black D (1980) *The manners and customs of the police*. New York: Academic Press
- Bowers KJ, Johnson SD, Pease K (2004) Prospective hot-spotting: The future of crime mapping? *Br J Criminol* 44(5):641–658, DOI 10.1093/bjc/azh036
- Braga A, Papachristos A, Hureau D (2012) Hot spots policing effects on crime. *Campbell Syst Rev* 8(8):1–96, DOI 10.4073/csr.2012.8
- Braga AA (2005) Hot spots policing and crime prevention: A systematic review of randomized controlled trials. *J Exp Criminol* 1(3):317–342, DOI 10.1007/s11292-005-8133-z
- Braga AA (2007) Policing crime hot spots. In: *Preventing Crime*, New York: Springer Publishing, pp 179–192, DOI 10.1007/1-4020-4244-2_12
- Braga AA, Weisburd D (2010) *Policing problem places: Crime hot spots and effective prevention*. Oxford: Oxford University Press
- Braga AA, Papachristos AV, Hureau DM (2010) The concentration and stability of gun violence at micro places in Boston, 1980–2008. *J Quant Criminol* 26(1):33–53, DOI 10.1007/s10940-009-9082-x
- Braga AA, Papachristos AV, Hureau DM (2014) The effects of hot spots policing on crime: An updated systematic review and meta-analysis. *Justice Q* 31(4):633–663, DOI 10.1080/07418825.2012.673632
- Camacho-Collados M, Liberatore F (2015) A decision support system for predictive police patrolling. *Decis Support Syst* 75:25–37, DOI 10.1016/j.dss.2015.04.012
- Carroll BW, Ostlie DA (2013) *An introduction to modern astrophysics*, 2nd edn. London: Pearson
- Chainey S, Tompson L, Uhlig S (2008a) The utility of hotspot mapping for predicting spatial patterns of crime. *Secur J* 21(1-2):4–28, DOI 10.1057/palgrave.sj.8350066

- Chainey S, Tompson L, Uhlig S (2008b) The utility of hotspot mapping for predicting spatial patterns of crime. *Secur J* 21(1):4–28, DOI 10.1057/palgrave.sj.8350066
- Chawathe SS (2007) Organizing hot-spot police patrol routes. In: 2007 IEEE Intelligence and Security Informatics, pp 79–86, DOI 10.1109/ISI.2007.379538
- Chen YC, Genovese CR, Wasserman L (2013) Uncertainty measures and limiting distributions for filament estimation. arXiv e-prints arXiv:1312.2098
- Chen YC, Genovese CR, Wasserman L (2015a) Asymptotic theory for density ridges. *Ann Stat* 43(5):1896–1928
- Chen YC, Ho S, Freeman PE, Genovese CR, Wasserman L (2015b) Cosmic web reconstruction through density ridges: Method and algorithm. *Mon Notices Royal Astron Soc* 454:1140–1156, DOI 10.1093/mnras/stv1996
- Chen YC, Ho S, Tenneti A, Mandelbaum R, Croft R, DiMatteo T, Freeman PE, Genovese CR, Wasserman L (2015c) Investigating galaxy-filament alignments in hydrodynamic simulations using density ridges. *Mon Notices Royal Astron Soc* 454:3341–3350, DOI 10.1093/mnras/stv2260
- Chen YC, Ho S, Brinkmann J, Freeman PEP, Wasserman L (2016) Cosmic web reconstruction through density ridges: Catalogue. *Mon Notices Royal Astron Soc* 461:3896–3909, DOI 10.1093/mnras/stw1554
- Chen YC, Ho S, Mandelbaum R, Bahcall NA, Brownstein JR, Freeman PE, Genovese CR, Schneider DP, Wasserman L (2017) Detecting effects of filaments on galaxy properties in the Sloan Digital Sky Survey III. *Mon Notices Royal Astron Soc* 466:1880–1893, DOI 10.1093/mnras/stw3127
- Chevaleyre Y (2004) Theoretical analysis of the multi-agent patrolling problem. In: Proceedings of the 2004 IEEE/WIC/ACM International Conference on Intelligent Agent Technology, pp 302–308, DOI 10.1109/IAT.2004.1342959
- Chevaleyre Y, Sempe F, Ramalho G (2004) A theoretical analysis of multi-agent patrolling strategies. In: Proceedings of the 3rd International Joint Conference on Autonomous Agents and Multiagent Systems, vol 4, pp 1524–1525, DOI 10.1109/AAMAS.2004.34
- Chrisman NR (2017) Calculating on a round planet. *International Journal of Geographical Information Science* 31(4):637–657, DOI 10.1080/13658816.2016.1215466
- Cohen LE, Felson M (1979) Social change and crime rate trends: A routine activity approach. *Am Sociol Rev* pp 588–608
- Cover TM, Hart PE (1967) Nearest neighbor pattern classification. *IEEE Trans Inf Theory* 13(1):21–27, DOI 10.1109/TIT.1967.1053964
- Eck JE, Chainey S, Cameron JG, Leitner M, Wilson RE (2005) Mapping crime: Understanding hot spots, 1st edn. Washington, D.C.: Office of Justice Programs, National Institute of Justice
- Fukunaga K, Hostetler LD (1975) The estimation of the gradient of a density function, with applications in pattern recognition. *IEEE Trans Inf Theory* 21(1):32–40, DOI 10.1109/TIT.1975.1055330
- Furtado V, Melo A, Menezes R, Belchior M (2006) Using self-organization in an agent framework to model criminal activity in response to police patrol routes. In: Proceedings of the 2006 Florida Artificial Intelligence Research Society Conference, pp 68–73
- Genovese CR, Perone-Pacifico M, Verdinelli I, Wasserman L (2012) The geometry of nonparametric filament estimation. *J Am Stat Assoc* 107(498):788–799, DOI 10.1080/01621459.2012.682527
- Genovese CR, Perone-Pacifico M, Verdinelli I, Wasserman L (2014) Nonparametric ridge estimation. *Ann Statist* 42(4):1511–1545, DOI 10.1214/14-AOS1218
- Ghassabeh YA, Linder T, Takahara G (2013) On some convergence properties of the subspace constrained mean shift. *Pattern Recognit* 46(11):3140–3147, DOI 10.1016/j.patcog.2013.04.014
- Griffith DA (2005) Effective geographic sample size in the presence of spatial autocorrelation. *Ann Am Assoc Geogr* 95(4):740–760, DOI 10.1111/j.1467-8306.2005.00484.x
- Groff ER, Weisburd D, Yang SM (2010) Is it important to examine crime trends at a local “micro” level?: A longitudinal analysis of street to street variability in crime trajectories. *J Quant Criminol* 26(1):7–32, DOI 10.1007/s10940-009-9081-y
- Haberman CP (2017) Overlapping hot spots? Examination of the spatial heterogeneity of hot spots of different crime types. *Criminol Public Policy* 16(2):633–660, DOI 10.1111/1745-9133.12303
- He S, Alam S, Ferraro S, Chen YC, Ho S (2017) The detection of the imprint of filaments on cosmic microwave background lensing. *Nat Astron* 2(5):401–406, DOI 10.1038/s41550-018-0426-z
- Hendel D, Johnston KV, Patra RK, Sen B (2018) A machine-vision method for automatic classification of stellar halo substructure. arXiv e-prints arXiv:1811.10613

- Hubble EP (1929) A relation between distance and radial velocity among extra-galactic nebulae. *Proc Natl Acad Sci USA* 15:168–173, DOI 10.1073/pnas.15.3.168
- Inman JW (1835) *Navigation and nautical astronomy for the use of British seamen*, 3rd edn. London: W. Woodward, C. & J. Rivington
- Kaashki NN, Safabakhsh R (2018) RGB-D face recognition under various conditions via 3D constrained local model. *J Vis Comm Image Represent* 52:66–85, DOI 10.1016/j.jvcir.2018.02.003
- Koper CS (1995) Just enough police presence: Reducing crime and disorderly behavior by optimizing patrol time in crime hot spots. *Justice Q* 12(4):649–672, DOI 10.1080/07418829500096231
- Leigh J, Dunnett S, Jackson L (2017) Predictive police patrolling to target hotspots and cover response demand. *Ann Oper Res* pp 1–16, DOI 10.1007/s10479-017-2528-x
- Li B, Griffith DA, Becker B (2016) Spatially simplified scatterplots for large raster datasets. *Geo Spat Inf Sci* 19(2):81–93, DOI 10.1080/10095020.2016.1179441
- Li K, Kwong S (2014) A general framework for evolutionary multiobjective optimization via manifold learning. *Neurocomputing* 146:65–74, DOI 10.1016/j.neucom.2014.03.070
- Li L, Jiang Z, Duan N, Dong W, Hu K, Sun W (2011) Police patrol service optimization based on the spatial pattern of hotspots. In: *Proceedings of the 2011 IEEE International Conference on Service Operations, Logistics and Informatics*, pp 45–50, DOI 10.1109/SOLI.2011.5986526
- Linning SJ, Eck JE (2017) Weak intervention backfire and criminal hormesis: Why some otherwise effective crime prevention interventions can fail at low doses. *Br J Criminol* 58(2):309–331, DOI 10.1093/bjc/azx019
- Mamalian CA, La Vigne NG, et al (1999) *The use of computerized crime mapping by law enforcement: Survey results*. Washington, D.C.: U.S. Dept. of Justice, Office of Justice Programs, National Institute of Justice
- Marchant R, Lu D, Cripps S (2018) Cox Bayesian optimization for police patrolling. In: *32nd Annual Conference on Neural Information Processing Systems*
- McGill R, Tukey JW, Larsen WA (1978) Variations of box plots. *Am Stat* 32(1):12–16
- Melo A, Belchior M, Furtado V (2005) Analyzing police patrol routes by simulating the physical reorganization of agents. In: *International Workshop on Multi-Agent Systems and Agent-Based Simulation*, pp 99–114, DOI 10.1007/11734680_8
- Menton C (2008) Bicycle patrols: An underutilized resource. *Policing* 31(1):93–108, DOI 10.1108/13639510810852594
- Miao Z, Wang B, Shi W, Wu H (2014) A method for accurate road centerline extraction from a classified image. *IEEE J Sel Top Appl Earth Obs Remote Sens* 7(12):4762–4771, DOI 10.1109/JSTARS.2014.2309613
- Ozertem U, Erdogmus D (2011) Locally defined principal curves and surfaces. *J Mach Learn Res* 12:1249–1286
- Paruchuri P, Pearce JP, Marecki J, Tambe M, Ordonez F, Kraus S (2008) Playing games for security: An efficient exact algorithm for solving Bayesian Stackelberg games. In: *Proceedings of the 7th International Joint Conference on Autonomous Agents and Multiagent Systems*, Vol. 2, pp 895–902
- Parzen E (1962) On estimation of a probability density function and mode. *Ann Math Statist* 33(3):1065–1076, DOI 10.1214/aoms/1177704472
- Qiao W, Polonik W (2016) Theoretical analysis of nonparametric filament estimation. *Ann Statist* 44(3):1269–1297, DOI 10.1214/15-AOS1405
- Ratcliffe J (2010) Crime mapping: Spatial and temporal challenges. In: *Handbook of quantitative criminology*, New York: Springer Publishing, pp 5–24, DOI 10.1007/978-0-387-77650-7_2
- Ratcliffe JH (2004) Crime mapping and the training needs of law enforcement. *Eur J Crim Policy Res* 10(1):65–83, DOI 10.1023/B:CRIM.0000037550.40559.1c
- Ratcliffe JH, Taniguchi T, Groff ER, Wood JD (2011) The Philadelphia foot patrol experiment: A randomized controlled trial of police patrol effectiveness in violent crime hotspots. *Criminology* 49(3):795–831, DOI 10.1111/j.1745-9125.2011.00240.x
- Reid ST (1979) *Crime and criminology*, 2nd edn. New York: Holt, Rinehart & Winston
- Reis D, Melo A, Coelho AL, Furtado V (2006) GAPatrol: An evolutionary multiagent approach for the automatic definition of hotspots and patrol routes. In: *Advances in Artificial Intelligence - IBERAMIA-SBIA 2006*, New York: Springer Publishing, pp 118–127, DOI 10.1007/11874850_16
- Rosenblatt M (1956) Remarks on some nonparametric estimates of a density function. *Ann Math Statist* 27(3):832–837, DOI 10.1214/aoms/1177728190

- Saragih JM, Lucey S, Cohn JF (2009) Face alignment through subspace constrained mean-shifts. In: 2009 IEEE 12th International Conference on Computer Vision, pp 1034–1041
- Sherman LW, Weisburd D (1995) General deterrent effects of police patrol in crime “hot spots”: A randomized, controlled trial. *Justice Q* 12(4):625–648, DOI 10.1080/07418829500096221
- Sherman LW, Gartin PR, Buerger ME (1989) Hot spots of predatory crime: Routine activities and the criminology of place. *Criminology* 27(1):27–56, DOI 10.1111/j.1745-9125.1989.tb00862.x
- Shreve M, Brizzi J, Fefilatyeve S, Luguev T, Goldgof D, Sarkar S (2014) Automatic expression spotting in videos. *Image Vis Comput* 32(8):476–486, DOI 10.1016/j.imavis.2014.04.010
- Slocum LA, Taylor TJ, Brick BT, Esbensen FA (2010) Neighborhood structural characteristics, individual-level attitudes, and youths’ crime reporting intentions. *Criminology* 48(4):1063–1100, DOI 10.1111/j.1745-9125.2010.00212.x
- Telep CW, Mitchell RJ, Weisburd D (2014) How much time should the police spend at crime hot spots? Answers from a police agency directed randomized field trial in Sacramento, California. *Justice Q* 31(5):905–933, DOI 10.1080/07418825.2012.710645
- Wasserman L (2018) Topological data analysis. *Annu Rev Stat Appl* 5(1):501–532, DOI 10.1146/annurev-statistics-031017-100045
- Weisburd D (2015) The law of crime concentration and the criminology of place. *Criminology* 53(2):133–157, DOI 10.1111/1745-9125.12070
- Weisburd D, Braga AA (2019) *Police innovation: Contrasting perspectives*. Cambridge: Cambridge University Press
- Weisburd D, Lum C (2005) The diffusion of computerized crime mapping in policing: Linking research and practice. *Police Pract Res* 6(5):419–434, DOI 10.1080/15614260500433004
- Weisburd D, Telep CW (2011) The efficiency of place-based policing. In: *Evidence-Based Policing*, Antwerpen: Maklu Publishers, pp 247–262, DOI 10.2139/ssrn.2630369
- Weisburd D, Bushway S, Lum C, Yang SM (2004) Trajectories of crime at places: A longitudinal study of street segments in the city of Seattle. *Criminology* 42(2):283–322, DOI 10.1111/j.1745-9125.2004.tb00521.x
- Wilcox P, Eck JE (2011) Criminology of the unpopular: Implications for policy aimed at payday lending facilities. *Criminol Public Policy* 10:473, DOI 10.1111/j.1745-9133.2011.00721.x
- Williamson D, McLafferty S, Goldsmith V, Mallenkopf J, McGuire P (1999) A better method to smooth crime incident data. *ESRI ArcUser Magazine* January–March 1999:1–5
- Xie M, Lauritsen JL (2012) Racial context and crime reporting: A test of Black’s stratification hypothesis. *J Quant Criminol* 28(2):265–293, DOI 10.1007/s10940-011-9140-z
- York DG, et al (2000) The Sloan Digital Sky Survey: Technical summary. *Astron J* 120(3):1579–1587, DOI 10.1086/301513
- Zamzmi G, Ruiz G, Shreve M, Goldgof D, Kasturi R, Sarkar S (2018) A method to suppress facial expression in posed and spontaneous videos. arXiv e-prints arXiv:1810.02401